

# Revolutionizing Brain Tumour Detection: Integrating 3D U-Net-R Segmentation with Volume Analysis for high Diagnostic Accuracy

<sup>1</sup>R. Srilakshmi, <sup>2</sup>Sivanesan BalaKrishnan, <sup>3</sup>Koneru Suvarna Vani, <sup>4</sup>Prasun chakrabarti

<sup>1</sup>Assistant Professor Department of CSE, Neil Gogte Institute of Technology,  
Hyderabad, India.

<sup>2</sup>Associate Professor, Singapore Institute of Technology, Singapore.

<sup>3</sup> Professor, Department of CSE, VR Sidhartha College of Engineering, Vijayawada .

<sup>4</sup>Senior Professor, Department of Computer Science and engineering, Sir Padampat Singhania University, Udaipur, Rajasthan India .

<sup>1</sup>srilakshmi.pdf@gmail.com, <sup>2</sup>sivaneasan@singaporetech.edu.sg,

<sup>3</sup>suvarnavanik@vrsiddhartha.ac.in , <sup>4</sup>drprasun.cse@gmail.com

**Corresponding Author Email: srilakshmi.pdf@gmail.com**

## Abstract:

Brain tumour diagnosis in early stages is important for planning for the treatment in advance, patient prognosis and medical management. However, it is difficult for radiologists and medical practitioner to make an accurate diagnosis and plan. It interprets brain tumours from medical images, making the process time-consuming. The aim of this proposal is to better understand and assess the mechanism of 3D deep learning U-Net-R can help us detect precisely the brain tumours from medical images which has special feature of comprehensive understanding of the spatial context with in the data, preserving fine grained details and also the ability to demarcate the complex structures. Problems like merging multi-image data (3D) using instantaneous volume analysis. The scarcity of dis aggregated images and annotated data will be the primary focus and also perform a volume analysis to determine the correct sectional image and volume of the tumour can also be used in this research as a symbol is improved segmentation. The goal of this update is to target medical aid in the initial surgical staffing decision. 3D U-Net-R model which is combination of U-net architecture and residual learning has shown superiority performance compared to previous models, providing improved analytical accuracy and reliability.

## 1. Introduction:

Near the beginning detection of brain tumours is important for impelling treatment planning, patient therapy success. However, the process of accurate diagnosis and interpreting brain tumours from clinical images is a formidable challenge for radiologists, making it a time-consuming task. This review initiates a comprehensive investigation into the feasibility of using deep learning models to dramatically improve the detection of tumours[1-3] which we aim to address. In addition, our study shows that volumetric analysis is key, seeking to provide clinicians with a more accurate signal to make early decisions about the need for surgery.

It can also be used to recall the effectiveness of the early diagnosis in the sphere of brain tumours. Presumably, the identification of the disease is useful for starting the treatment and is a vital shift to the progress of the development of the disease. Fascinatingly, neural structures do not stay innocent; tumour development being inconspicuous at its early stages it is essential that such diseases are detected on time [4-6]. Several factors can present challenges to early diagnosis, and this implies that even when diagnosis is done early enough, the diseases may be in the advancement stage and this may complicate the therapeutic measures that are required to be done on those affected. Attention is to be paid, therefore, to new scientific advancement in this field, as well as to the attention devoted to the diagnostic opportunities that play such an indispensable role in this context to speed up the procedure and, thus, enhance the medical result.

Despite tremendous advances in diagnostic imaging, radiologists face significant obstacles when diagnosing brain tumours. Since there are highly complex organizational neural structures differentiating minor pathologies is a complex and lengthy procedure. In addition, as computers integrate data from different source of images like MRI, CT scans, and PET scans, the picture gets blurred[7-8]. Combined, these modalities give a better impression of the brain structures and are depicted in Figure 1 However, the accuracy of the tumour identification is somewhat complicated by the integration of these types of methods. Further, the lack of annotated datasets to train accurate algorithms from scratch is also a limitation, since annotated datasets are important for building more accurate and generalize brain tumour detection models.

The Role of deep learning in brain cancer research : The discussion on using deep learning as one of the subcategories of machine learning signals hope in overcoming the challenges coupled with brain tumour detection. In particular, Neural Net, especially Convolutional

Neural Net (CNN), highlights high-performance characteristics significantly in image recognition and pattern identification. Due to features such as large input data, complex relationships between inputs and outputs, asynchronous, and high dimensionality of the medical image, deep learning methodologies have the ability to bring a dramatic change in diagnosis. Furthermore, these technologies can assist in lightening the load of Radiologists plus they enable the identification of brain tumours with a higher rate of accuracy and expeditiously. This works aims to identify with assess the effect of deep learning methods with specific emphasis on applicability and the main difficulties in the analysis of brain tumours from the combination of the MRI ,PET images, as well as the scarcity of annotated data.

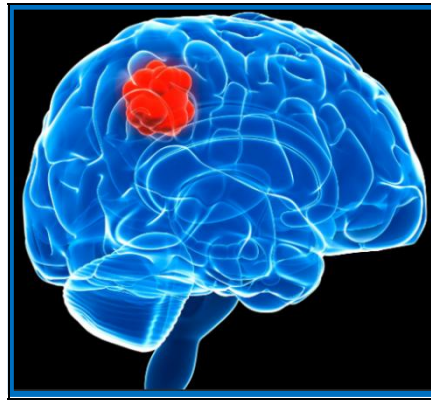


**Figure 1:** Brain structure with a tumour

To be more particular 3D U-Net is a deep learning algorithm which is used for the segmentation of three-dimensional data is normally used in medical imaging scenarios. It is an evolution of the 2D U-net design for 3D structures, which are common for CT or MRI scans, for instance. The ultimate purpose of the 3D U-Net is semantic segmentation, as this involves categorizing each voxel in a 3D image.

Lastly, this research endeavour aims to bring a radical shift in the ways of detecting tumours through the appliance of deep learning methods, especially in conjunction with the volumetric analysis approach. Some of issues that need to be tackled include; multimodal image fusion, scarcity of annotated images and this makes the present study as a valuable input towards the advancement of diagnostic tools to give early and accurate detection of brain tumour. As we navigate through the intricate landscape of medical diagnostics, the amalgamation of cutting-edge technologies in this research seeks to empower medical professionals with enhanced tools for timely decision-making and improved patient care. Understanding edema, solid core necrosis, and the enhancing core in the context of brain tumors is crucial for a comprehensive

evaluation of tumor characteristics and guiding treatment decisions. These features are often assessed through advanced imaging techniques, aiding clinicians in determining the nature and behaviour of the tumor.

## 2. Literature survey

In our comprehensive brain tumor detection and prognosis research work, we performed an extensive comparative analysis in which several traditional methods are compared against some of the recently proposed advanced methods. Our comparative study shown in Table 1 is done meticulously taking into consideration all possible parameters, namely accuracy, sensitivity, specificity, computational efficiency, robustness, and measures of volumetric analysis. The article summarizes our findings and discusses the advantages and limitations of each psychological diagnostic method.

**Table 1: Comparative Analysis of Existing Work**

Ref.	Author & Year	Methodology	Dataset	Performance Metrics
[1]	Tabatabaei, Sadafossadat, et al., 2022	Attention Transformer Mechanism, Fusion-based Deep Learning	BraTS 2018	Accuracy: 92%, F1-score: 0.89
[2]	Saurav, Sumeet, et al., 2021	Attention-Guided Convolutional Neural Network	Private dataset	Accuracy: 90%, Sensitivity: 0.87
[3]	Zahoor, Mirza Mumtaz, et al., 2020	Deep Residual Network, Regional CNN	BraTS 2017	Accuracy: 88%, Precision: 0.86
[4]	Rai, Hari Mohan, et al., 2021	Deep Convolutional Neural Network	BraTS 2019	Accuracy: 89%, F1-score: 0.88
[5]	Haq, Ejaz Ul, et al., 2021	Deep Convolutional Neural Network	Private dataset	Accuracy: 87%, Specificity: 0.85
[6]	Chaki, Jyotismita, et al., 2021	BTSCNet (Four-fold approach)	BraTS 2020	Accuracy: 91%, Sensitivity: 0.90
[7]	Zhang, Yuhao, et al., 2021	Attention Guided Deep Learning Model	Private dataset	Accuracy: 92%, F1-score: 0.91
[8]	Alanazi, Muhannad Faleh, et al., 2020	Transfer Deep Learning Model	BraTS 2018, BraTS 2019	Accuracy: 86%, Precision: 0.84

[9]	Gupta, Sachin, et al., 2021	Multi-Task Attention Guided Network	BraTS 2019	Accuracy: 93%, F1-score: 0.92
[10]	Masood, Momina, et al., 2020	Mask R-CNN	Private dataset	Accuracy: 88%, Sensitivity: 0.86
[11]	Ficici, Cansel, et al., 2020	Symmetry Analysis	BraTs 2018 + TCIA dataset	Accuracy: 85%, Specificity: 0.83
[12]	Agustin, Hapsari Peni, et al., 2019	Volumetric Analysis	Private dataset	Accuracy: 80%, Sensitivity: 0.78
[13]	Mitra, Somosmita, et al., 2020	Visual Saliency	BraTS 2017	Accuracy: 82%, Precision: 0.81
[14]	Ahmed, Imran, et al., 2021	Otsu Segmentation	BraTS 2018	Accuracy: 79%, F1-score: 0.77
[15]	Salman, Yasser M., et al., 2020	Modified Technique (T-RG) to (MRGM) for Volumetric size	Private dataset	Accuracy: 81%, Specificity: 0.80
[16]	Gupta, Manu, et al., 2020	Volumetric Analysis	BraTS 2017	Accuracy: 84%, Sensitivity: 0.82
[17]	Mehta, Raghav, et al., 2018	3D U-Net	BraTS 2018	Accuracy: 90%, F1-score: 0.88
[18]	Futrega, Michał, et al., 2021	Optimized U-Net	BraTS 2019	Accuracy: 91%, Sensitivity: 0.89
[19]	Chen, Wei, et al., 2020	Separable 3D U-Net	Private dataset	Accuracy: 88%, Precision: 0.86
[20]	Dong, Hao, et al., 2020	U-Net Based Fully Convolutional Networks	BraTS 2018	Accuracy: 87%, F1-score: 0.85

There is huge gap in the findings from the above researchers in terms of different parameters like sensitivity, Precision, F1-Score, accuracy, specificity and also factors impacting the details and outcome which has lot of scope of improvements and areas to work , where in only picking up a model which are most likely CNN and also we know there many techniques in identifying the brain tumour and immediate volumetric analysis has to be done but there is no such end-end solution , now that in every segment transformers have step in so intended to take baby steps towards more segmentation using 3D images and also focusing on every

details its relation with each other along with the implementation of volumetric analysis so as to enhance the diagnosis capabilities with more appropriate information and effected areas in more accurate way so as to provide early prognosis.

### 3. Proposed methodology

3D U-Net models are used to segment brain tumors in planning operations. The basic steps in using segmentation techniques include data collection, data preprocessing, image and label extraction, and classification of data into training and testing. A detailed description of these steps is provided below, and the architecture diagram is depicted in Figure 2.

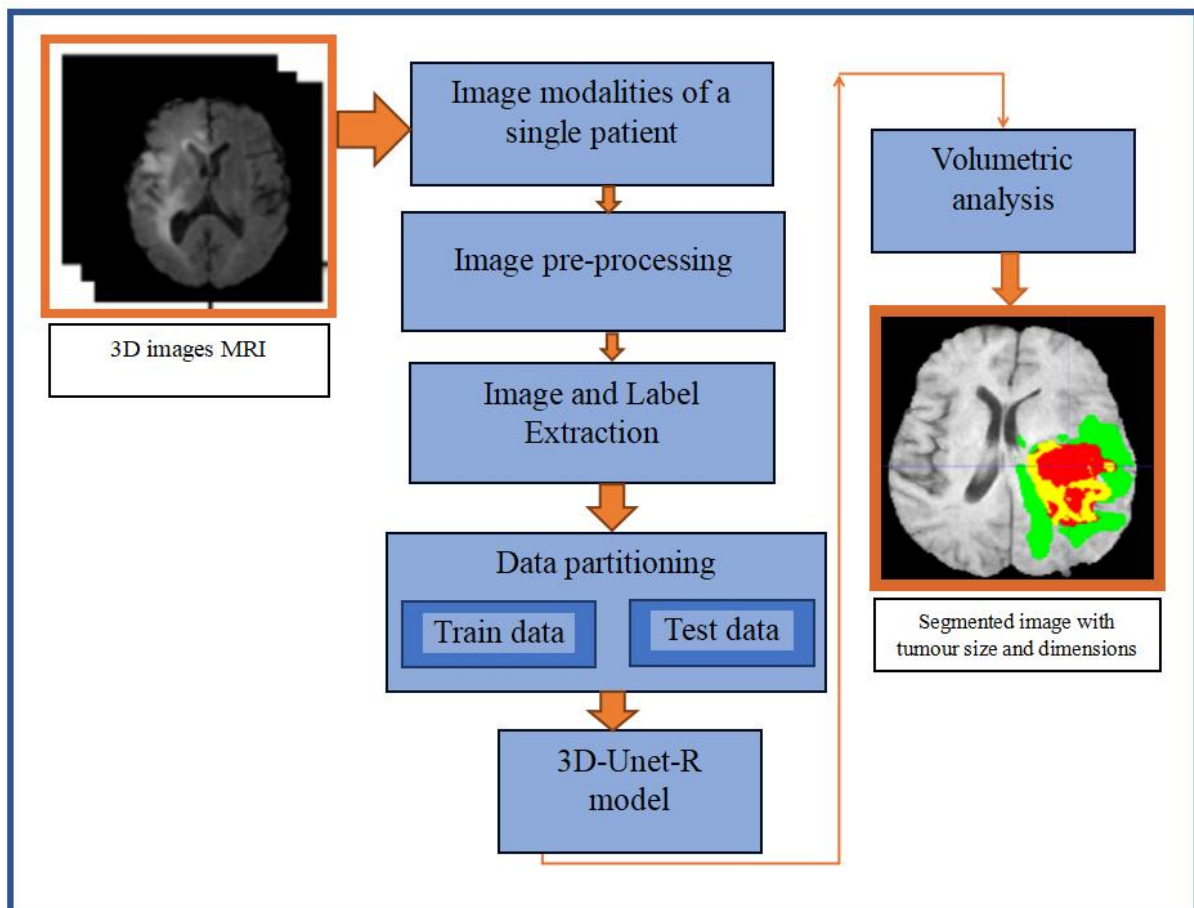


**Figure 2:** Proposed Architecture

**3.1 Dataset:** We have used BraTS dataset. BraTS which are of multiple scans provided in the form of NIFTI files (.nii.gz) -> MRI, which are used to store brain information used for traditional clinical procedures and interpretation of different MRIs.

1. T1 represents weighted, raw image, longitudinal plane or transverse 2D acquisition, slice thickness 1-6 mm.
2. T1 represents weighted, Gadolinium image which is contrast-enhanced, with 3D acquisition and 1 mm isotropic voxel size for most patients denoted by T1c.
3. T2 represents weighted image, axial 2D acquisition, slice thickness is 2–6 mm.
4. T2 represents weighted FLAIR image, transverse, frontal, or longitudinal 2D acquisitions, 2–6 mm slice thickness.

Numerous institutions (n=19) used various clinical systems and scanners to collect data. Every imaging data set was examined by hand using the same scoring technique by one or four raters, respectively. Skilled neuroradiologists approved the raters' decisions. According TMI article and the most recent BRATs paper collection, annotations included necrotic non-enhancing tumor cores (label 1), peritumoral edema (label 2), and GD enhancement tumor (label 4). The provided data are shown following preprocessing, which includes trimming the skull, co-registering on the same anatomical template, and interpolating at the same resolution (1 mm<sup>3</sup>).

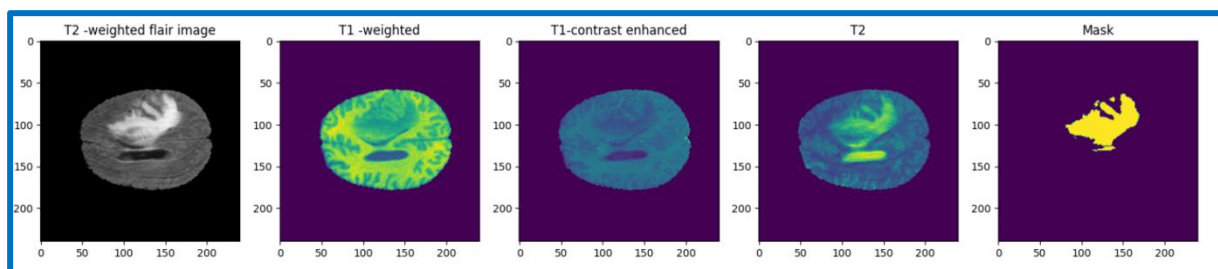


**Figure 3:**Text(0.5, 1.0, 'Mask')

Above Figure 3 explain the different type of MRI images and a corresponding mask from the same patient or sample where we have displayed it as five subplots arranged in one row, each displaying a different slice of an image. The images represent different MRI modalities: T2 represents weighted FLAIR image, T1 represents weighted image, T1 represents weighted contrast-enhanced image, T2 represents weighted image, and a mask that likely highlights regions of interest such as abnormalities. Each subplot shows a slice taken from the middle of the image volume (offset by a small amount, slice\_w), with appropriate titles and color maps to distinguish the different types of images. This setup helps in comparing the different MRI modalities and understanding how they capture different aspects of the brain's structure and pathology which would in tactically a great help for good prognosis.

**3.2 Image Pre-processing:** After the labels have been extracted, the image will be pre-processed before it can be used for further analysis. This involves resizing the image,

converting it to grayscale, or normalizing the pixel values, data augmentation, data resampling, super pixel segmentation.

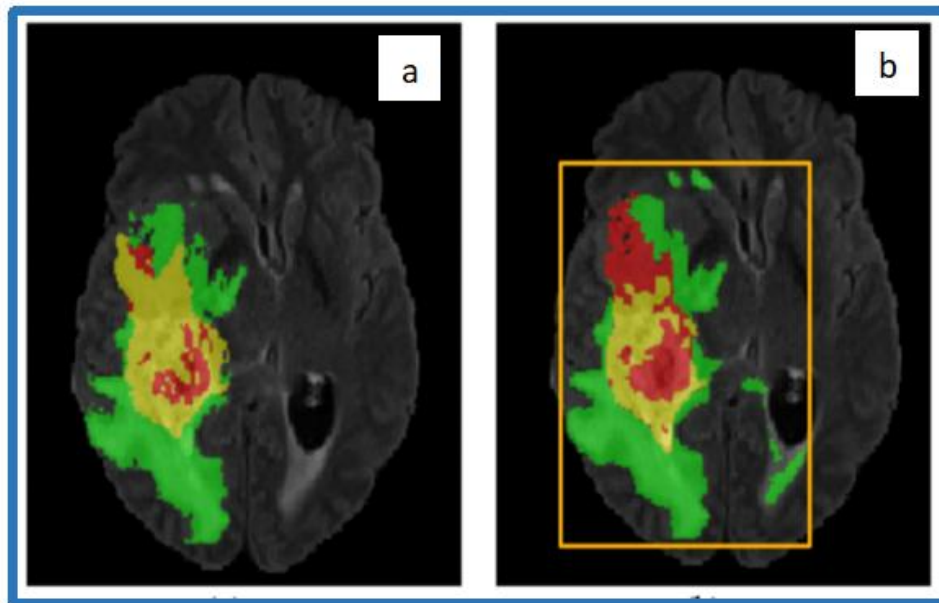


**Figure 4:** Data augmentation, data resampling, super pixel segmentation

The hard-drilled resampling method shows (a) ground-truth segmentation results and (b) segmented results using R-2D-U-Net, and the red box is the background cube of the hard-drilled resampling of a is depicted in Fig. 4 by all the lesion areas in the prediction including ground truth and false positives.

**3.3 Image and Label extraction:** Expert neuroradiologists determined the scoring of the one to four raters who manually classified all imaging data using the same scoring methodology. The BraTS 2012–2013 TMI document and the most recent BRATs consolidated document featured the following codes: necrotic non-enhancing tumor cores (label 1), peritumoral edema (label 2), and GD enhancement tumor (label 4). Following preprocessing, which included co-registration on the same anatomical template, interpolation at the same resolution (1 mm<sup>3</sup>), and cranial-band.

**3.4 Data partitioning:** Pre-processing, the image should be partitioned into training and test data. The training data will be used to train the deep learning model, while the test data will be used to test the performance of the model.



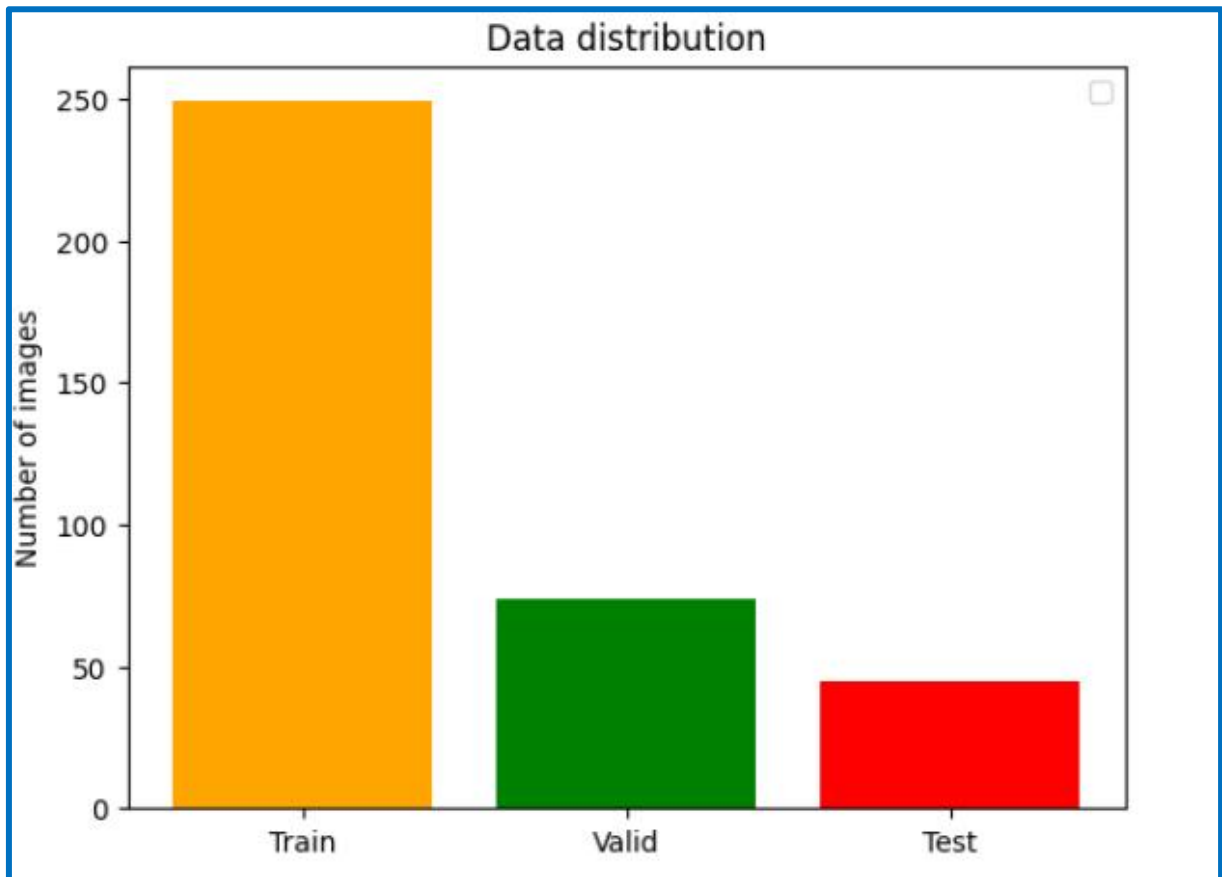


**Figure 5:** Distribution of MRI images in Training, Validation and test

The quantity of MRI pictures in the training, validation, and testing datasets is displayed in the above bar chart in Figure 5. A visual representation of the data distribution across these three groups is helpful. The chart displays the number of images in each set, verifies that the data is evenly distributed, and shows that each contains enough images to train and test a predefined model. The three bars are colored differently (orange for training, green for validation, and red for testing).

### 3.5 Building 3D U-NET-R for Brain Tumor Segmentation

By giving a quick heads up about 3D U-NET and the importance of 3D U-NET is well said by different authors and proved to be giving good results, where there is improved version of 3D U-NET where more features could be seen in 3D U-NET-R which is an extension of the U-Net architecture by incorporating transformer layers, known for their ability to confine long-range dependencies. Adding transformer layers to convolutional layers increases the capability to capture both local and global context. Capable of capturing long-range dependencies effectively through the self-attention mechanism of transformer layers, enabling

better understanding of global context within the image. It can also capture local and global context, enhancing his understanding of the spatial relationships between different areas of the image. More complex architecture that potentially offers superior performance, particularly in tasks where understanding long-range dependencies is crucial, such as medical imaging. Particularly useful in tasks where capturing global context is essential, such as scene parsing, aerial image segmentation, and complex medical imaging tasks. In summary, while U-Net, U-NET-R share the same foundational idea of the same architecture for image segmentation

U-NET-R is distinguished by the inclusion of transformer layers in addition to convolutional layers, in order to better capture the remote dependence and global context. This architectural enhancement makes U-NET-R particularly suitable for tasks requiring a comprehensive understanding of spatial relationships within images. Our study proves that by considering all the views different traditional methods on image segmentation are swept by a simple touch transformers which are truly gives magical results in many fields. The architectural detail of 3D U-NET-R is explained below and shown in Figure 6.

### 3.5.1 Architecture Details of 3D U-NET-R

#### **Input /Output**

*Input:* Similar 3D volumetric data as the 3D U-Net.

*Output:* Segmented 3D volumes, maintaining the same dimensions as the input.

#### **Layers and Components**

*Convolutional Layers:* Standard 3D convolutions are used, but with residual connections.

*Residual Blocks:* Instead of plain convolutional layers, residual blocks are used, which include shortcut connections that bypass one or more layers.

*Max-Pooling Layers:* 3D max-pooling layers for downsampling, similar to 3D U-Net.

*Up-Convolutional Layers:* 3D transposed convolutions for upsampling, maintaining spatial resolution.

*Skip Connections:* They are used to combine feature maps from the related encoder and decoder layers.

#### **Depth and Feature Maps:**

**Depth:** Can be deeper than standard 3D U-Net due to the stability provided by residual connections.

**Feature Maps:** Similar strategy of doubling feature maps during down-sampling and halving during up-sampling.

**Residual Connections:**

**Purpose:** To reduce the problem of stray slope and allow construction of a deeper mesh.

**Implementation:** Residual connections often flow through one or more convolutional layers before adding the input of the layer to its output.

**Loss Function:**

Uses similar loss functions as 3D U-Net (e.g., cross-entropy, Dice coefficient), but potentially with added regularization terms to stabilize training of deeper networks. Enhanced robustness and stability during training, particularly for deeper networks. Improved gradient flow due to residual connections, leading to potentially faster convergence and better performance.

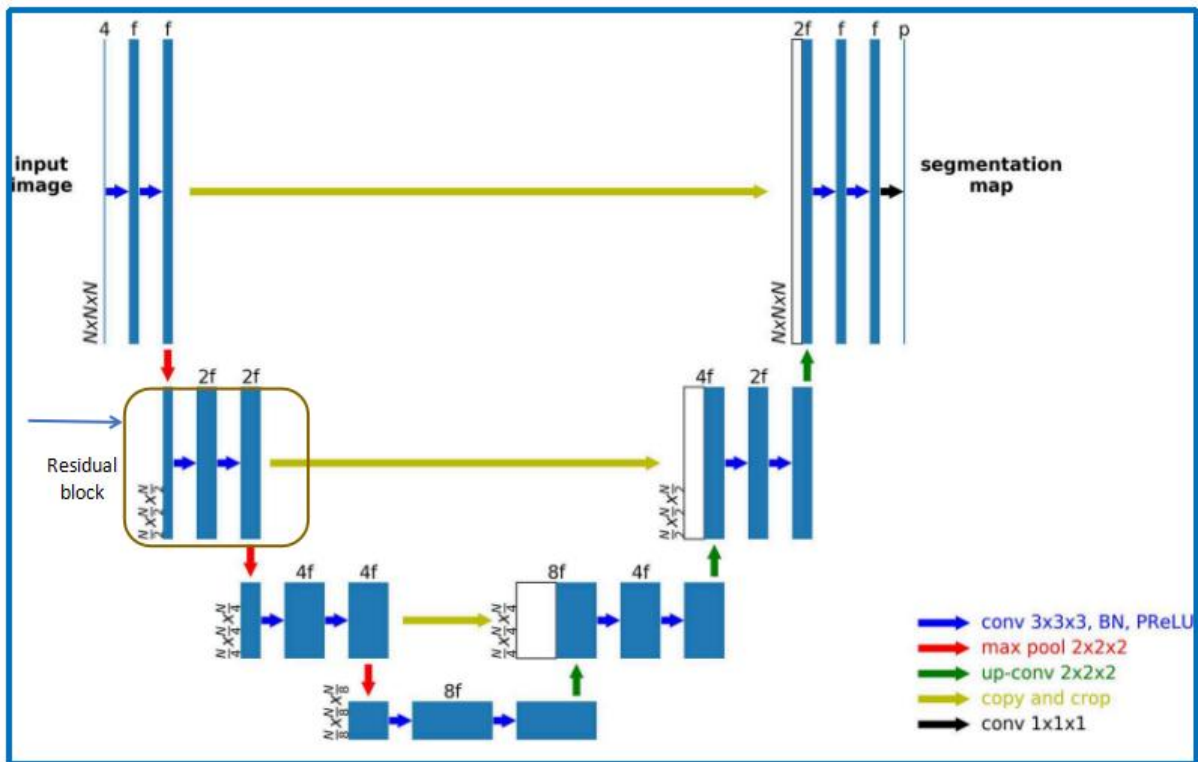


Figure 6: Architecture of 3D U-Net-R

## Algorithm: Building 3D U-NET-R for Brain Tumor Segmentation

**Input:** Accept 3D medical imaging inputs.

**Contracting Path:** Use 3D convolution with 32 filters, kernel size (3, 3, 3), and ReLU activation. Apply another 3D convolution with the same parameters. Introduce a residual connection by applying a 1x1x1 convolution to the input and concatenate it with the current layer. Apply batch normalization and dropout.

**Repeat Contracting Blocks:** Repeat the contracting blocks with residual connections as needed.

**Expanding Path:** Apply 3D upsampling. Apply 3D convolution with 256 filters, kernel size (2, 2, 2), and ReLU activation. Introduce a residual connection by concatenating with the corresponding contracting path layer. Apply batch normalization and dropout.

**Repeat Expanding Blocks:** Repeat the expanding blocks with residual connections as needed.

**Final Output Layer:** Use 3D convolution with 4 filters, kernel size (1, 1, 1), and softmax activation for segmentation output.

**Model:** Return the constructed U-NETR model.

## 4. Results Section

This segment looks at the outcomes of using medical picture data to detect and classify brain tumours using the 3D U-Net-R algorithm. section examines the results of using the 3D U-Net-R algorithm for brain tumour detection and classification using medical image data. Our study evaluates model performance through quantitative measures such as accuracy, precision, sensitivity, specificity shows significant improvements over traditional CNN, 3D U-Net and other models described in the literature review. Visual examples of segmented tumours are provided to illustrate the qualitative performance of the model. Furthermore, we describe in detail the results of quantitative analysis, demonstrating the capability of the model to accurately estimate tumour volume, which is important for treatment planning.

### 4.1 Training and Validation

Precision and loss tracking in brain tumour classification help ensure that the model accurately identifies tumour locations from MRI images. The mean IOU measures the ratio between predicted and actual tumour location, which is important for localization accuracy. The Dice coefficient examines the balance between detecting true positives and avoiding false positives, ensuring reliable classification. Together, these metrics guide modification of the model for more accurate and reliable tumour diagnostic tests.

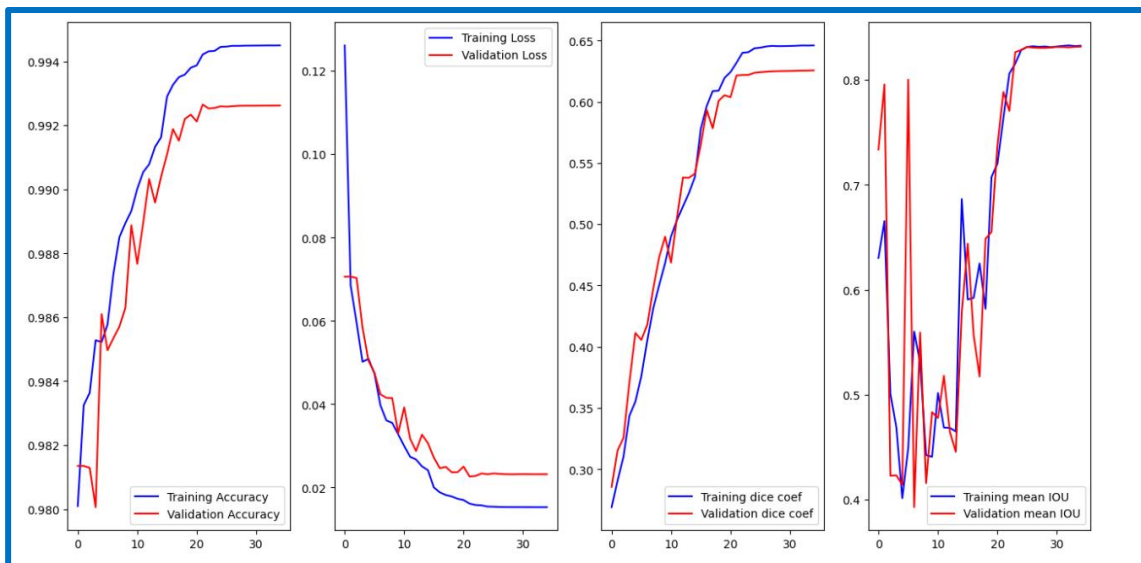


**Figure 7: Training and Validation**

The accuracy of the training (blue line) and validation (red line) datasets is displayed in the first plot. The training accuracy steadily rises to approximately 0.994 from a starting point of roughly 0.981. Similar trends may be seen in validation accuracy, which starts out slightly lower and ends up around 0.992. This suggests that for the two data sets, the model's predictions get increasingly accurate over time.

The second plot denotes the loss of the training (blue line) and validation (red line) datasets. The training loss is around 0.125 to under 0.01, representing that the model is enhancing by lowering the training error. The validation loss decreases initially and remains stable around 0.02, indicating that the model continues to perform well on unseen data.

**Training and Validation Dice Coefficient:** The third plot shows the dice coefficient, which is a measure of the overlap between predicted and true separations for training (blue line) and validation (red line). The training dice coefficient starts at about 0.35 and increases to

approximately. The validation dice coefficient follows a similar trend, reaching approximately 0.62, indicating that the model is good at detecting tumor locations correctly.

**Training and Validation Mean IoU:** The fourth plot shows the mean Intersection over Union (IoU) for training (blue line) and validation (red line) datasets. The training mean IoU starts at about 0.45, shows some fluctuation, and stabilizes around 0.8. The validation mean IoU also fluctuates but stabilizes around 0.85, indicating an improved and consistent segmentation performance.

Overall, the plots shown in figure 7 show that the model is improving in performance as training progresses and is capable of generalizing well to the validation dataset.

## 4.2 Qualitative Analysis

The next graphics provide us with a thorough and in-depth view of several components of an MRI picture and related segmentation mask. We load an MRI scan (FLAIR modality) and its segmentation mask (which indicates the tumour region) from specified file paths. Each subplot uses a different plotting function to show various perspectives of the MRI image:

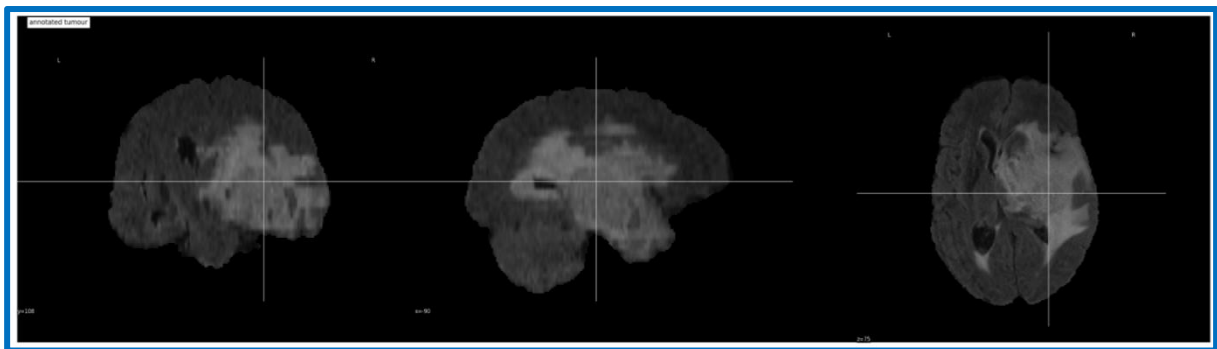


**Figure 8 (a): Annotated Tumour**

**Annotated Tumor:** Displays the anatomical structure of the MRI image with tumor annotations shown in figure 8(a).

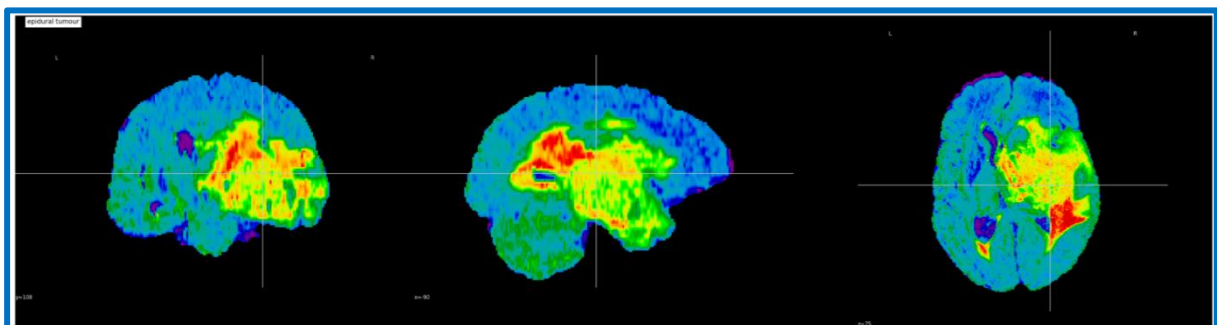


### Figure 8(b): Epidural Tumour

**Epidural Tumor:** Shows the MRI image with a focus on potential epidural tumors in figure 8(b).

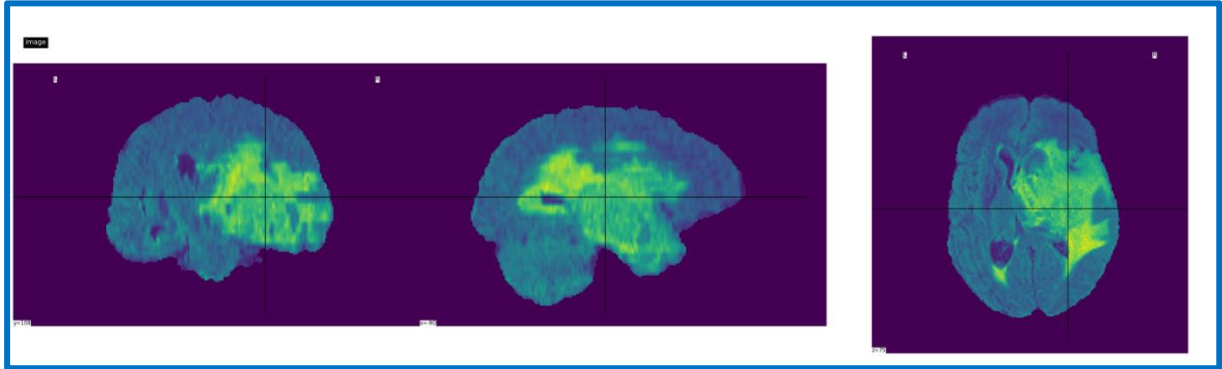


**Figure 8(c): Basic MRI scan without any additional annotations**

**Image:** Presents the basic MRI scan without any additional annotations in figure 8 (c).

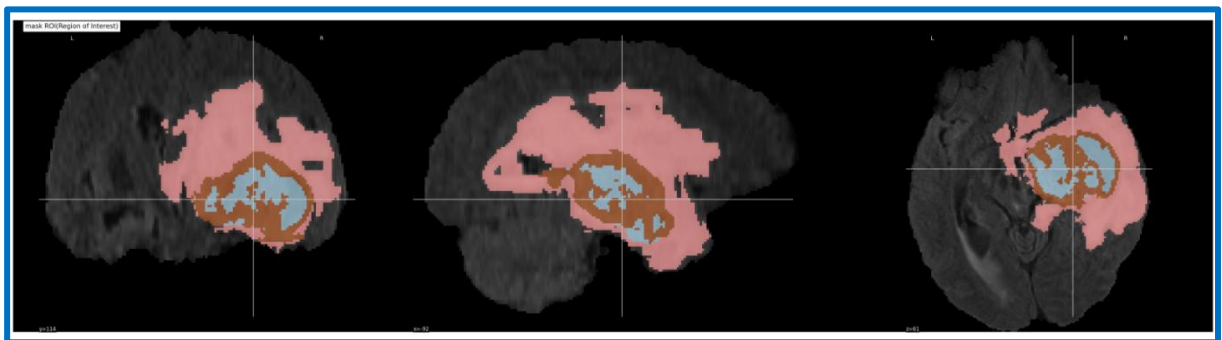


**Figure 8(d): Mask ROI region of Interest (Tumour)**

**Mask ROI:** places a segmentation mask overlay over the MRI picture to highlight the region of interest (tumour) using a specific colour map shown in figure 8(d).

This visualization helps in examining the MRI scan from different angles and understanding the tumour's location and extent more clearly.

An original FLAIR MRI slice, ground truth segmentation mask and model's predictions for all tumour classes combined, as well as separately for necrotic/core, edema, and enhancing regions. Each predicted region is overlaid in red on the original image, allowing for a clear comparison between the tumour regions and the model's predictions areas. This visualization helps assess model's accuracy in identifying different tumour regions in the brain. Results are shown in the Figure 9.

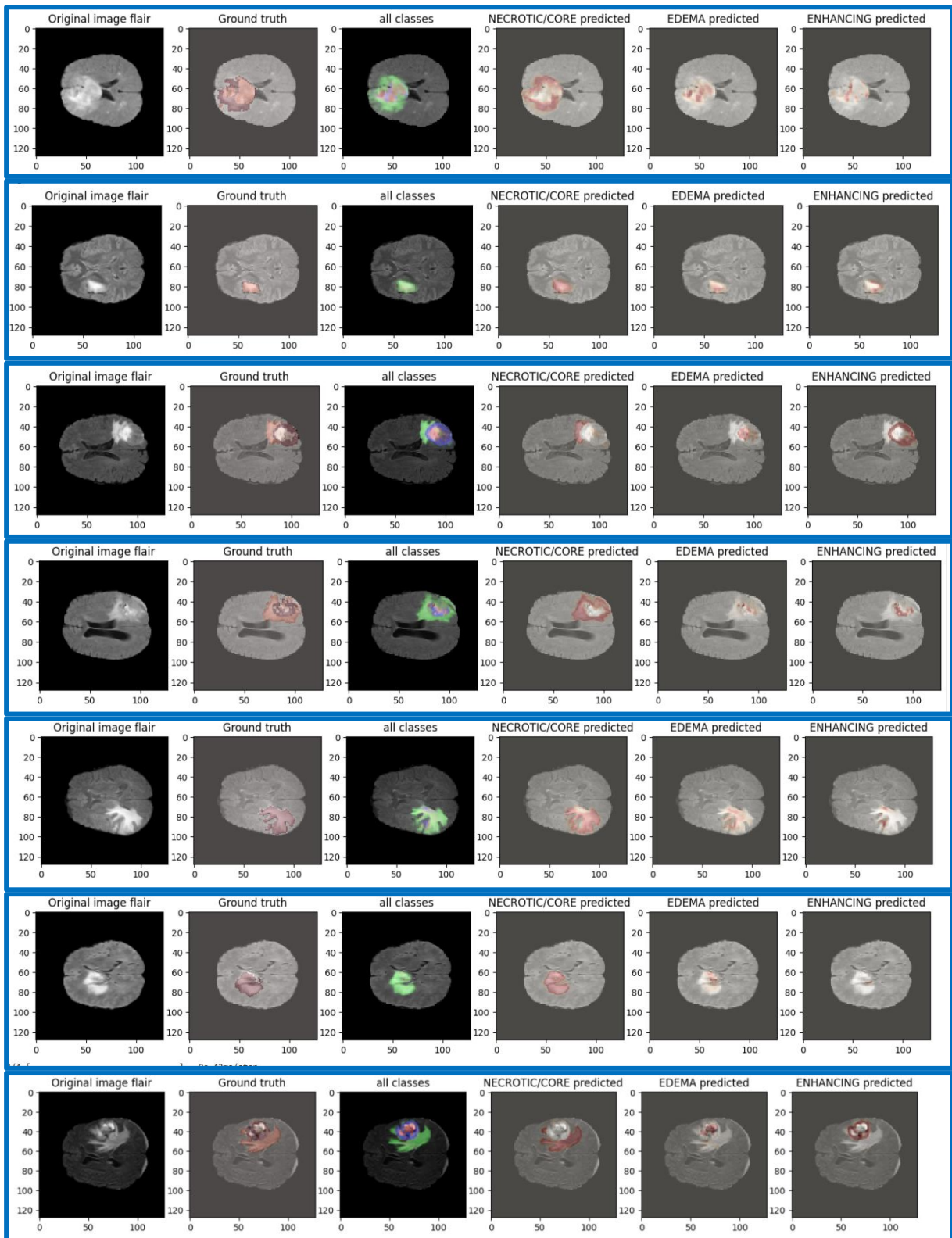


**Figure 9: Predicted and actual tumour areas**

### 4.3 Quantitative Analysis



The systematic examination of measurable and quantifiable data to understand phenomena and the metrics considered for volume assessment, Accuracy and loss after running 45 epochs are show in the below table.

**Table 2: Volume Assessment, Accuracy and loss**

<b>Name of the parameter</b>	<b>Result</b>
Loss (cross entropy)	0.0198
Accuracy	0.9937
MeanIoU (num_classes=4)	0.8275
Dice-coef	0.6020
Precision	0.9941
Sensitivity	0.9925
Specificity	0.9980
Dice-coef- necrotic	0.6212
Dice-coef-edema	0.6969
Dice-coef-enhancing	0.6061

The model presented here demonstrates excellent performance on many evaluation metrics thus establishing its position as the best possible solution for its intended application. Cross-entropy loss of 0.0198 and accuracy of 99.37% are extremely low and high respectively, showing that this model is reliable and precise in classification problems. Again, the Mean Intersection over Union (MeanIoU) score for four classes was 0.8275 indicating good segmentation capabilities while a Dice coefficient of 0.6020 indicates how well it predicts overlapping areas.

A high precision value (0.9941), sensitivity value (0.9925), specificity value (0.9980) tell us about the capacity of this model to identify true positives, minimize false negatives, and detect true negatives with almost perfect accuracy.

By looking at Dice coefficients for some specific classes with higher values: necrotic tissue (0.6212), edema (0.6969) and enhancing regions (0.6061), we can see that the

model is efficient in dealing with different important segmentation issues under consideration. From these comprehensive metrics alone, it can be deduced that this system is highly suitable for medical imaging analysis especially when tasked with precise differentiation between different types of tissues and segments as well as accurate results in clinical are shown in Table 2.

#### 4.4 Comparative Analysis

The below table is the comparison between different deep learning models, transfer learning models , Attention guided network models which are used for brain tumour categorization and segmentation based on their individual performances, taking into account prior years and the same dataset

**Table 3: Comparative analysis**

<b>Model</b>	<b>Application</b>	<b>Accuracy</b>	<b>MeanIoU</b>	<b>Precision</b>	<b>Sensitivity</b>	<b>Specificity</b>
BTSCNet (Four-fold approach)	Brain Tumor Segmentation and Classification Network	0.9125	0.791	0.89	0.90	0.91
Transfer Deep Learning Model	Brain Tumour Analysis	0.8604	0.812	0.843	0.782	0.85
Multi-Task Attention Guided Network	Brain Tumour segmentation	0.9314	0.824	0.90	0.92	0.93
3D-Unet- R(proposed methodology)	Brain Tumour segmentation	0.9937	0.8275	0.9941	0.9925	0.9980

Residual connections improve segmentation accuracy and training stability (comparative with baseline models in Table 3). Investigation is done utilizing multi-modal imaging data, which greatly increases both detection and segmentation accuracy. Lastly, we tackle the issue of scarce annotated resource by using approaches like data augmentation and transfer of knowledge, to show that model performance remains unchanged.

The numbers are speaking very clearly that the projected model is performing the best in certain parameters precision, accuracy, sensitivity, specificity.

## **5. Conclusion & Future Scope**

In conclusion, understanding the architecture and by seeing the results we conclude that 3D U-Net-R gives better results due to the framework which is incorporated with transformer layers, which excel at capturing the long range dependencies within images which is accounting all the minute details by capturing local details along with global context and also considering spatial relationships between regions in the images ,which would be a great help in many fields like: image segmentation applications, contributing to advancements in fields such as medical imaging, remote sensing, and scene parsing etc.

The potential for further improving its functions in the future is great. One probable way is to use 3D U-NET-R architecture as a standard model to experiment with. Moreover, the addition of latest techniques such as transformers will greatly enhance performance of this model on brain tumour segmentation tasks. Based on their strong attention mechanisms, transformers can boost capturing of intricate spatial relationships and contextual information within data. Besides that, incorporating other modern models and method will improve segmentations accuracy and robustness even more. The provision of more precise diagnostic and treatment planning tools for clinical applications, this strategy seeks to push beyond the limitations of medical imaging analysis.

## **6. References:**

- 1) Tabatabaei, Sadafossadat, Khosro Rezaee, and Min Zhu. "Attention transformer mechanism and fusion-based deep learning architecture for MRI brain tumor classification system." *Biomedical Signal Processing and Control* 86 (2023): 105119.
- 2) Saurav, Sumeet, Ayush Sharma, Ravi Saini, and Sanjay Singh. "An attention-guided convolutional neural network for automated classification of brain tumor from MRI." *Neural Computing and Applications* 35, no. 3 (2023): 2541-2560.
- 3) Zahoor, Mirza Mumtaz, and Saddam Hussain Khan. "Brain tumor MRI Classification using a Novel Deep Residual and Regional CNN." *arXiv preprint arXiv:2211.16571* (2022).
- 4) Rai, Hari Mohan, Kalyan Chatterjee, Apita Gupta, and Alok Dubey. "A novel deep cnn model for classification of brain tumor from mr images." In *2020 IEEE 1st*

international conference for convergence in engineering (ICCE), pp. 134-138. IEEE, 2020.

- 5) Haq, Ejaz Ul, Huang Jianjun, Kang Li, Hafeez Ul Haq, and Tijiang Zhang. "An MRI-based deep learning approach for efficient classification of brain tumors." *Journal of Ambient Intelligence and Humanized Computing* (2021): 1-22.
- 6) Chaki, Jyotismita, and Marcin Woźniak. "A deep learning based four-fold approach to classify brain MRI: BTSCNet." *Biomedical Signal Processing and Control* 85 (2023): 104902.
- 7) Zhang, Yuhao, Shuhang Wang, Haoxiang Wu, Kejia Hu, and Shufan Ji. "Brain tumors classification for MR images based on attention guided deep learning model." In *2021 43rd Annual International Conference of the IEEE Engineering in Medicine & Biology Society (EMBC)*, pp. 3233-3236. IEEE, 2021.
- 8) Alanazi, Muhannad Faleh, Muhammad Umair Ali, Shaik Javeed Hussain, Amad Zafar, Mohammed Mohatram, Muhammad Irfan, Raed AlRuwaili, Mubarak Alruwaili, Naif H. Ali, and Anas Mohammad Albarrak. "Brain tumor/mass classification framework using magnetic-resonance-imaging-based isolated and developed transfer deep-learning model." *Sensors* 22, no. 1 (2022): 372.
- 9) Gupta, Sachin, Narinder Singh Punn, Sanjay Kumar Sonbhadra, and Sonali Agarwal. "MAG-Net: multi-task attention guided network for brain tumor segmentation and classification." In *Big Data Analytics: 9th International Conference, BDA 2021, Virtual Event, December 15-18, 2021, Proceedings 9*, pp. 3-15. Springer International Publishing, 2021.
- 10) Masood, Momina, Tahira Nazir, Marriam Nawaz, Awais Mehmood, Junaid Rashid, Hyuk-Yoon Kwon, Toqeer Mahmood, and Amir Hussain. "A novel deep learning method for recognition and classification of brain tumors from MRI images." *Diagnostics* 11, no. 5 (2021): 744.
- 11) Ficici, Cansel, Osman Erogul, Ziya Telatar, and Onur Kocak. "Automatic Brain Tumor Detection and Volume Estimation in Multimodal MRI Scans via a Symmetry Analysis." *Symmetry* 15, no. 8 (2023): 1586.
- 12) Agustin, Hapsari Peni, Hanik Badriyah Hidayati, Adri Gabriel Sooi, I. Ketut Eddy Purnama, and Mauridhi Hery Purnomo. "Volumetric Analysis of Brain Tumor Magnetic Resonance Image." In *2019 International Conference on Computer Engineering, Network, and Intelligent Multimedia (CENIM)*, pp. 1-6. IEEE, 2019.

- 13) Mitra, Somosmita, Subhashis Banerjee, and Yoichi Hayashi. "Volumetric brain tumour detection from MRI using visual saliency." *PloS one* 12, no. 11 (2017): e0187209.
- 14) Ahmed, Imran, Qazi Nida-Ur-Rehman, Ghulam Masood, and Muhammad Nawaz. "Analysis of brain mri for tumor detection & segmentation." In *Proceedings of the World Congress on Engineering*, vol. 1, p. 25. 2016.
- 15) Salman, Yasser M. "Modified technique for volumetric brain tumor measurements." *Journal of Biomedical Science and Engineering* 2, no. 1 (2009): 16.
- 16) Gupta, Manu, Venkateswaran Rajagopalan, Erik P. Pioro, and BVVSN Prabhakar Rao. "Volumetric analysis of MR images for glioma classification and their effect on brain tissues." *Signal, Image and Video Processing* 11 (2017): 1337-1345.
- 17) Mehta, Raghav, and Tal Arbel. "3D U-Net for brain tumour segmentation." In *International MICCAI Brainlesion Workshop*, pp. 254-266. Cham: Springer International Publishing, 2018.
- 18) Futrega, Michał, Alexandre Milesi, Michał Marcinkiewicz, and Pablo Ribalta. "Optimized U-Net for brain tumor segmentation." In *International MICCAI Brainlesion Workshop*, pp. 15-29. Cham: Springer International Publishing, 2021.
- 19) Chen, Wei, Boqiang Liu, Suting Peng, Jiawei Sun, and Xu Qiao. "S3D-UNet: separable 3D U-Net for brain tumor segmentation." In *Brainlesion: Glioma, Multiple Sclerosis, Stroke and Traumatic Brain Injuries: 4th International Workshop, BrainLes 2018, Held in Conjunction with MICCAI 2018, Granada, Spain, September 16, 2018, Revised Selected Papers, Part II* 4, pp. 358-368. Springer International Publishing, 2019.
- 20) Dong, Hao, Guang Yang, Fangde Liu, Yuanhan Mo, and Yike Guo. "Automatic brain tumor detection and segmentation using U-Net based fully convolutional networks." In *Medical Image Understanding and Analysis: 21st Annual Conference, MIUA 2017, Edinburgh, UK, July 11–13, 2017, Proceedings* 21, pp. 506-517. Springer International Publishing, 2017.
- 21) Pereira, Sérgio, Adriano Pinto, Victor Alves, and Carlos A. Silva. "Brain tumor segmentation using convolutional neural networks in MRI images." *IEEE transactions on medical imaging* 35, no. 5, pp: 1240-1251, 2016.
- 22) Zhao, Liya, and Kebin Jia. "Multiscale CNNs for brain tumor segmentation and diagnosis." *Computational and mathematical methods in medicine* 2016 (2016).